Fragile altermagnetism and orbital disorder in Mott insulator $LaTiO_3$

I. V. Maznichenko,[1,2,*] A. Ernst,[3,4] D. Maryenko,[5] V. K. Dugaev,[6] E. Ya. Sherman,[7,8] P. Buczek,[1] S. S. P. Parkin,[4] and S. Ostanin[2]

[1]*Department of Engineering and Computer Sciences, Hamburg University of Applied Sciences, Berliner Tor 7, D-20099 Hamburg, Germany*
[2]*Institute of Physics, Martin Luther University Halle-Wittenberg, D-06099 Halle, Germany*
[3]*Institute for Theoretical Physics, Johannes Kepler University, A-4040 Linz, Austria*
[4]*Max Planck Institute for Microstructure Physics, Weinberg 2, D-06120 Halle, Germany*
[5]*RIKEN Center for Emergent Matter Science (CEMS), Wako 351-0198, Japan*
[6]*Department of Physics and Medical Engineering, Rzeszów University of Technology, 35-959 Rzeszów, Poland*
[7]*Department of Physical Chemistry and the EHU Quantum Center, University of the Basque Country UPV/EHU, Bilbao 48080, Spain*
[8]*Ikerbasque, Basque Foundation for Science, Bilbao 48009, Spain*

(Received 3 April 2024; accepted 23 May 2024; published 5 June 2024)

Based on *ab initio* calculations, we demonstrate that a Mott insulator $LaTiO_3$ (LTO), not inspected previously as an altermagnetic material, shows the characteristic features of altermagnets, i.e., (i) fully compensated antiferromagnetism and (ii) k-dependent spin-split electron bands in the absence of spin-orbit coupling. The altermagnetic ground state of LTO is protected by the crystal symmetry and specifically ordered d orbitals of Ti ions with the orbital momentum $l = 2$. The altermagnetism occurs when sites of Ti pairs in the unit cell are occupied by single electrons with $m = -1$, $s_z = +1/2$ and $m = +1$, $s_z = -1/2$ per site, with m and s_z- being the z-component of the orbital momentum and spin, respectively. By further simulating orbital disorder within the Green's function method, we disclose its damaging character on the spin splitting and the resulting altermagnetism. When the single-electron spin-polarized state at each Ti site is contributed almost equally by two or three t_{2g} orbitals, LTO becomes antiferromagnetic. The effect of the spin-orbit coupling, which can cause orbital disorder and suppress altermagnetism, is discussed.

DOI: 10.1103/PhysRevMaterials.8.064403

I. INTRODUCTION

Altermagnets (AM) are a subset of the large class of collinear antiferromagnetic materials which display no net magnetization yet which have k-dependent spin-split electronic bands. This is in contrast with conventional collinear antiferromagnets for which the up and down spin polarized bands are indistinguishable throughout k space [1–3]. Using *ab initio* electronic band structure calculations, within the density functional theory (DFT) and a nonrelativistic spin group formalism [4], more than a dozen candidate altermagnets have been proposed, including insulating fluorides (MnF_2), oxides (Fe_2O_3) and perovskites ($LaMnO_3$), chalcogenide semiconductors (MnTe), semimetals ($CoNb_3S_6$), and various metals (RuO_2, CrSb, Mn_5Si_3) [5,6]. The crystal and electronic structures of these proposed AMs, as well as their chemical compositions and properties, are diverse. Yet, all AMs exhibit time-reversal ($\mathcal{T}$) symmetry breaking which leads to a spin-split electronic structure in the absence of spin-orbit coupling [7]. This leads to a number of spin-dependent phenomena that make AMs of potential interest for spintronics applications [5,8]. For the case of RuO_2, the band structure predictions are supported by observations of an anomalous Hall effect [9], spin current and torque [10–12], as well as the observation of magnetic circular dichroism in angle-resolved photoemission spectroscopy (ARPES) [13]. AMs can show relatively high magnetic ordering temperatures T_{AM} and large spin splitting of the electronic bands which has stimulated experimental efforts to provide direct evidence of altermagnetism from ARPES measurements. Indeed, spin-splitting of the electronic bands in α-MnTe ($T_{\mathrm{AM}} = 267$ K) have been recently reported to be as much as ∼370 meV [14,15].

Here we consider the Mott insulator $LaTiO_3$ (LTO) that has not previously been calculated as an altermagnet, although the material meets needed requirements [3,5]. (i) LTO is orthorhombic with a unit cell that contains two antiferromagnetically G-ordered sublattices of Ti^{3+}. (ii) There is no inversion center between the Ti sites because of tilted TiO_6 octahedra. (iii) The opposite-spin sublattices are connected by translation combined with rotation. In LTO, the semiconducting band gap separates the occupied Ti $t_{2g}^1 e_g^0$ subband from the unoccupied conduction band edge, while the f states of La appear at much higher energies. The key structural factor of *Pbnm*-LTO, which determines its band gap and zero magnetization, is optimally rotated TiO_6 [16]. The symmetry of LTO does not differ from that of other ABO_3 potential altermagnets, such as $LaVO_3$ or $LaMnO_3$. However, the occupied Ti-based d subband in LTO contains one electron only, i.e., the lowest possible value. This single orbital filling enlarges the spin-split effects and their visibility in the bandstructure, producing a clear picture of the altermagnetism appearance.

*igor.maznichenko@physik.uni-halle.de

 ©2024 American Physical Society

In this work, we show from first principles calculations that orthorhombic LTO exhibits an altermagnetic band structure, focusing on the Ti d-orbital filling. In cubic LTO, there are three t_{2g} orbitals which can be occupied by one electron. Quantum effects such as a Jahn-Teller distortion and spin-orbit coupling can remove the t_{2g} degeneracy. Keimer *et al.* [17] reported that the orbital momentum of the t_{2g} level is quenched, and suggested a picture of strongly fluctuating t_{2g} orbitals. The observed anomalies were explained by assuming the formation of an orbital liquid state [18]. Keeping in mind the scenario of orbital fluctuations, we further present here simulations of orbital disorder, using a Green's function method. First of all, for the ordered and specifically filled Ti t_{2g} orbitals, our DFT calculations show a strongly split spin band. Then, to simulate orbital disorder, the charge of one electron was distributed among the two or three t_{2g} orbitals on each Ti site to show the important effects of orbital mixing on the spin splitting of the electron bands. We conclude that when at least two d orbitals of Ti become almost equally filled, altermagnetic LTO transforms into an antiferromagnet.

II. DETAILS OF CALCULATIONS

The electronic and magnetic properties of LTO were computed from first principles using the Korringa-Kohn-Rostoker (KKR) Green's function method [19,20] based on multiple scattering theory within the DFT and generalized gradient approximation [21] to the exchange-correlation potential. The full charge-density treatment used here takes into account a nonsphericity of both the crystal potential and charge density. The maximal angular momentum used was $l_{\max} = 3$ and the integrals over the Brillouin zone were performed using a $16 \times 16 \times 16$ k mesh.

For the AM configurations of LTO, the disordered filling of the Ti $(l = 2, m, s_z)$ states was simulated using the coherent potential approximation (CPA) [22–24]. The method adequately mimics homogeneously distributed disorder without a large supercell.

To reproduce the LTO properties within the DFT + U parametrization [25], correlation parameters U_{eff} of 2.3 eV and 6 eV, were applied to the Ti $3d$ states and f states of La, respectively. The D_{2h} magnetic unit cell of LTO, with four formula units (f.u.) in the a-b plane, is shown in Fig. 1. The cell allows the modeling of the TiO_6 octahedral tilting, antiferromagnetically ordered Ti and the altermagnetic band structure.

III. RESULTS AND DISCUSSION

The total spin-resolved density of states (DOS) and its site-projected components (PDOS) are shown in Fig. 2. A band gap of 0.22 eV separates the occupied Ti d subband from the unoccupied conduction bands, the bottom edge (E_c) of which is also formed by Ti orbitals. The f states of La appear well above E_c by +1.3 eV. Since each Ti^{3+} has an antiferromagnetically (AFM) ordered partner, we show in Fig. 2 only one Ti. According to our calculations, each Ti^{3+} has a magnetic moment with a value of ~ 0.8 μ_B.

First, we calculated all the ordered electronic configurations where only one t_{2g} orbital of each Ti is completely filled.

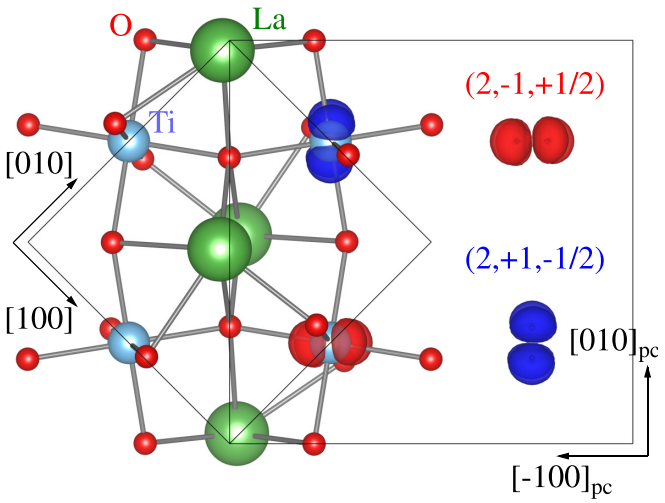

FIG. 1. Top view of the magnetic unit cell, $\sqrt{2}a \times \sqrt{2}b$, of orthorhombic $LaTiO_3$. The ordered and filled orbitals of a pair of Ti atoms ($l = 2, m = -1, s_z = +1/2$) and ($l = 2, m = +1, s_z = -1/2$) are shown, respectively, by red and blue color. The directions of the pseudocubic cell are labeled as "pc."

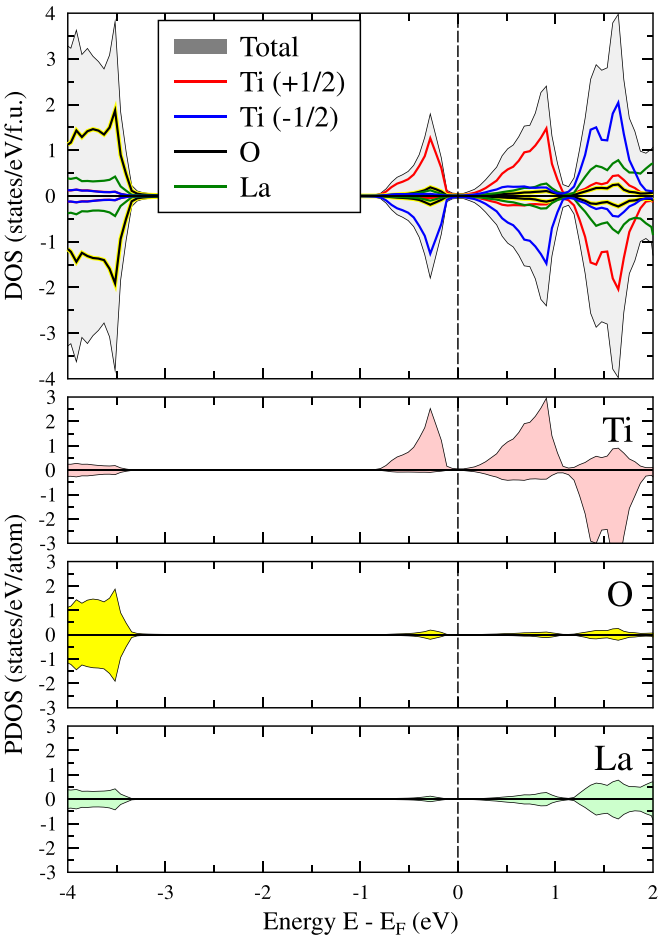

FIG. 2. The total spin-resolved density of states (DOS) and its site-projected components (PDOS) of orthorhombic $LaTiO_3$ per formula unit and per atom, respectively.

TABLE I. Total energies of LTO per formula unit, calculated for the FM, three AFM (*A*-, *C*- and *G*-type), three AM configurations, and the orbital-ordered (OO) FM configuration. Each energy value is shown with respect to the AM-*G* ground state. The one-orbital filled states (l, m, s_z) are given for each Ti pair.

Configuration	Filled states of Ti pair	Total energy (meV/f.u.)
AFM-*A*	(2,−2,+1/2),(2,−2,−1/2)	92.89
AFM-*C*	(2,−2,+1/2),(2,−2,−1/2)	114.60
AFM-*G*	(2,−2,+1/2),(2,−2,−1/2)	115.41
FM	(2,−2,+1/2),(2,−2,+1/2)	115.21
AM-*A*	(2,−1,+1/2),(2,+1,−1/2)	59.64
AM-*C*	(2,−1,+1/2),(2,+1,−1/2)	115.11
AM-*G*	(2,−1,+1/2),(2,+1,−1/2)	0.00
FM (OO)	(2,−1,+1/2),(2,+1,+1/2)	15.30

Since the $(l = 2, m, s_z)$ nomenclature is very suitable for the 3*d* Ti states of orthorhombic LTO, this orbital nomenclature is used below. For comparison, the Ti states $(2, m = -1, s_z)$ and $(2, m = +1, s_z)$ can be associated with those denoted in cubic perovskites as d_{xz} and d_{yz}, respectively. The nomenclature $(2, -2, s_z)$ corresponds to d_{xy}. The total energies computed for the three AM, FM, and three differently ordered AFM configurations of LTO are shown in Table I. By inspecting these energies we find that the *G*-type AM structure has the lowest energy. The AM-*A* and AM-*C* structures are not favorable energetically, as compared to that of AM-*G*. Additionally, to keep the 4-f.u.-cell LTO rigorously altermagnetic, the filled orbital nomenclature (l, m, s_z) of two Ti^{3+} should be $(2, -1, +1/2)$, while the one-orbital filling of two other Ti is $(2, +1, -1/2)$. Therefore, the ordered filling of the Ti t_{2g} orbitals with magnetic quantum numbers $m = \pm 1$ plays a key role for the emergence of AM in LTO. In Fig. 3, the non-relativistic total and spin-resolved Bloch spectral functions of energetically preferable AM-*G* configuration of LTO are plotted along the [110] and [−110] directions of the Brillouin zone (BZ). These correspond to $[100]_{pc}$ and $[010]_{pc}$ for the pseudocubic cell. We show in Fig. 3 the branches $E(\mathbf{k})$, which appear in the energy window of 2.4 eV around the Fermi level ($E_F = 0$). The low conduction bands of LTO, seen in Fig. 3,

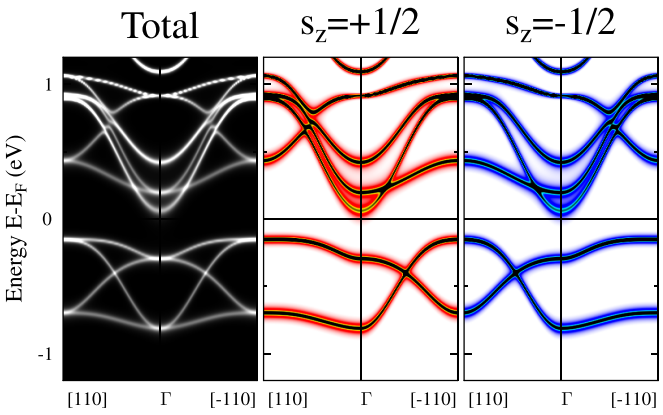

FIG. 3. Total and spin-resolved Bloch spectral functions of altermagnetic LTO, which are plotted along the [110] and [−110] k directions near $E_F = 0$ between $-1.2\,\text{eV} < E - E_F < +1.2\,\text{eV}$.

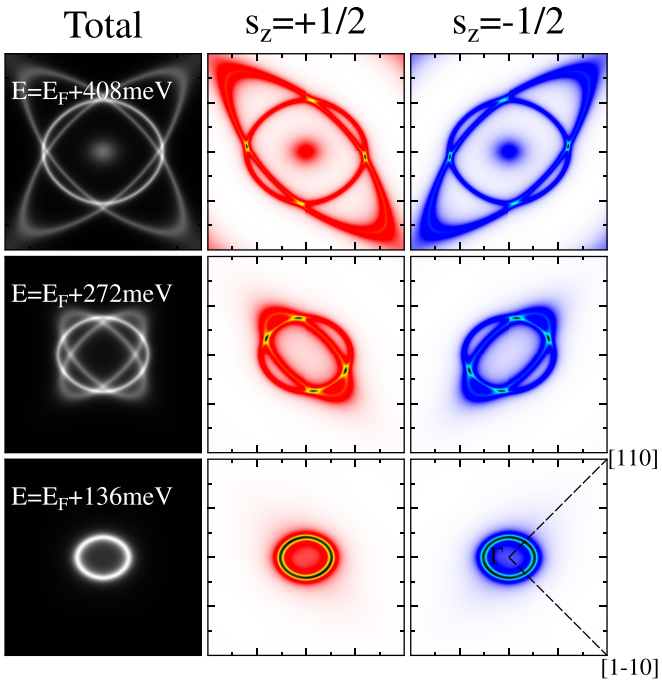

FIG. 4. Total and spin-resolved conduction-band cross sections of altermagnetic $LaTiO_3$, which were calculated within the BZ plane $k_z = 0$ at $E = E_F + 0.14\,\text{eV}$, $E = E_F + 0.27\,\text{eV}$, and $E = E_F + 0.41\,\text{eV}$.

above E_F are related solely to the unoccupied Ti 3*d* states. The bands seen in Fig. 3 below E_F represent the filled states $(l = 2, m = -1)$ for $s_z = +1/2$ and $(l = 2, m = +1)$ for $s_z = -1/2$. The total Bloch spectral function, plotted in the left panel of Fig. 3, shows that each $E(\mathbf{k})$ has spin degeneracy and gives an idea how the antiferromagnetic band structure of LaTiO3 looks like. For comparison, the two spin-resolved $E(\mathbf{k})$, which are plotted in the middle and right panels of Fig. 3, represent the spin-spin AM band structure. Within this approach, altermagnetism in LTO is strongly energetically favored. A narrow gap Mott insulator LTO can become conducting [26] without a strong modification of its crystal structure. The conductivity origins can include decreased tilting angles of TiO_6 octahedra [16], a small concentration of oxygen vacancies providing electron doping without distorting the structure, and an applied external bias. Here, for altermagnetic LTO, we mimic its hypothetical metallization by assuming that an external bias is applied. Cross sections of $E(\mathbf{k})$ within the BZ plane $k_z = 0$ are plotted in Fig. 4. At $E = E_F + 140\,\text{meV}$, the Fermi surface (FS) would consist of a few relatively small electron sheets closed around the BZ center Γ, as shown in the lower panels of Fig. 4. Then, with increasing bias voltage, all FS sheets enlarge and, simultaneously, extend along [1,1] and [−1, 1] within the $k_z = 0$ plane. For energies which exceed E_F by more than 0.3 eV, we find that the total FS has a fourfold symmetry, whereas each spin contributes to twofold sheets perpendicularly extended to eachother. The spin-resolved FS contour lines of altermagnetic LTO, which is shown in the upper panels of Fig. 4, suggests that rather strong in-plane anisotropy can appear in the spin-dependent conductivity at 0.3–0.4 eV above E_F. This is due to

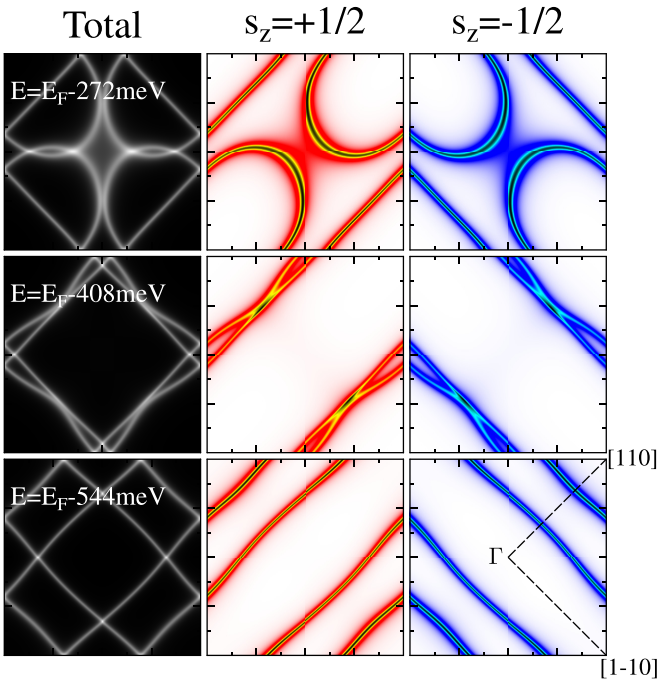

FIG. 5. Total and spin-resolved valence-band cross sections of altermagnetic $LaTiO_3$, which were calculated within the BZ plane $k_z = 0$ at $E = E_F - 0.27\,\text{eV}$, $E = E_F - 0.41\,\text{eV}$, and $E = E_F - 0.54\,\text{eV}$.

altermagnetism and appears when the bias or doping probes the conduction bands. It should be noted that the FS contour lines shown in Fig. 4 is related to the *Pbnm*-LTO (001) plane. The use of an appropriate shift of the Fermi level allows one to also consider the occupied Ti t_{2g} subband of altermagnetic LTO. Three valence-band cross sections, calculated within the BZ plane $k_z = 0$ at $E = E_F - 0.27\,\text{eV}$, $E = E_F - 0.41\,\text{eV}$, and $E = E_F - 0.54\,\text{eV}$, are plotted in Fig. 5. For each cut of $E(\mathbf{k})$, the total FS of fourfold symmetry includes spin-dependent contributions, each of which appears as open sheets of twofold symmetry. Since the spin-up and spin-down sheets are elongated perpendicularly to each other, as Fig. 5 shows, we expect that the in-plane spin transport in altermagnetic LTO might be highly anisotropic. Again, these predictions relate to the LTO (001) plane only.

Next, by simulating disorder for the Ti t_{2g} orbitals with the CPA method, we show the fragility of this altermagnetism due to multiorbital effects. This effects occur in the case of completely filled $(2, -1, +1/2)$ and $(2, +1, -1/2)$ orbitals for each Ti pair. Using the KKR-CPA technique, several electronic configurations with underfilled $(2, -1, +1/2)$ and $(2, +1, -1/2)$ were simulated. The missing charges were kept to take the $(2, -2, +1/2)$ and $(2, -2, -1/2)$ orbitals. The charge transfer, Δq, to the $(2, -2, \pm 1/2)$ orbitals varied from zero to 0.5 electron (e) on each Ti. The corresponding effect of the two equally filled Ti orbitals on the band structure of LTO is shown in Fig. 6. The well mixed electronic configuration calculated with $\Delta q = 0.5\,e$ illustrates explicitly the trends of the elimination of altermagnetism by multiorbital filling. One can expect that the main changes in $E(\mathbf{k})$ should take place below E_F, since the charge was redistributed between the

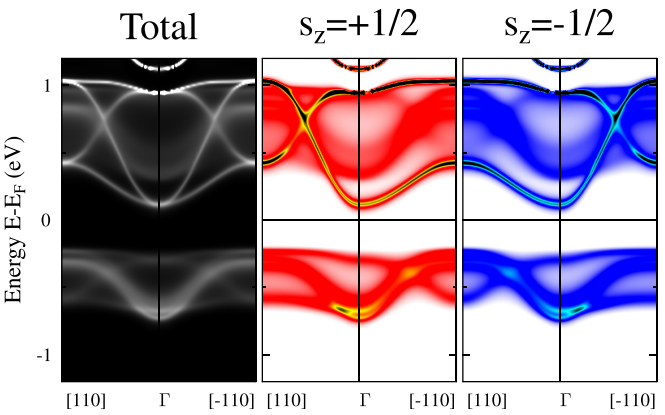

FIG. 6. Spin-resolved band structure of LTO, calculated with the two equally filled and disordered d orbitals on each Ti site. Here, the initially AM $(2,\pm1, \pm1/2)$ orbitals and initially AFM $(2,2,\pm1/2)$ orbitals of each Ti were mixed and filled by 0.5 e.

filled Ti orbitals only. Indeed, with increasing Δq, initially large spin splitting weakens. As Fig. 6 shows, when Δq approaches $0.5\,e$, the band structure of LTO below E_F is more conventionally antiferromagnetic than altermagnetic.

Finally, we simulated the case of completely disordered t_{2g} orbitals by taking three orbitals into consideration. The three orbitals of each Ti site, namely, $(2,-2, \pm1/2)$, $(2, 1,\pm1/2)$, and $(2,-1, \pm1/2)$ were filled equally by $1/3$. The corresponding spin-polarized band structure is plotted in Fig. 7 which shows that the material now becomes a conventional AFM.

The effects of orbital fluctuations, which can be triggered in LTO by spin-orbit coupling (SOC) were studied, e.g., in [17,18] prior to the nonrelativistic concept of altermagnetism in the absence of any SOC. Note that in our simulations, the SOC is also not considered. With inclusion of SOC, this relativistic effect renders spins and orbitals differently mixed for each electronic band state $E(\mathbf{k})$, thus permitting orbital fluctuations and making the SOC the main damaging factor of altermagnetism.

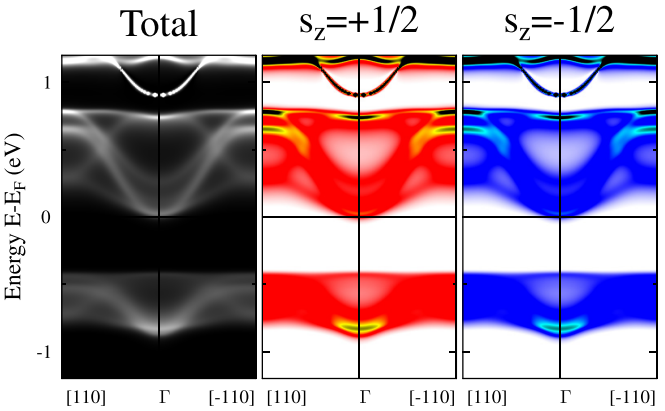

FIG. 7. Spin-resolved band structure of the AFM G-type LTO, calculated with the three equally filled by $1/3$ and disordered t_{2g} orbitals of each Ti.

IV. SUMMARY AND OUTLOOK

We presented *ab initio* calculations of altermagnetic $LaTiO_3$ performed with the Green's function method and coherent potential approximation. First, we found that the energetically preferable altermagnetic configuration is protected by the unit cell symmetry and, most importantly, by specifically filled Ti t_{2g} orbitals. For the Ti pairs in each unit cell, the single-electron electron states ($l = 2, m = -1, s_z = +1/2$) and ($l = 2, m = +1, s_z = -1/2$) per site should be filled. Second, we observed that orbital disorder damages the spin splitting and, therefore, destroys the altermagnetism. This happens when at least two orbitals, for instance, ($l = 2, m = \pm 1$) and ($l = 2, m = -2$), contribute equally to single-electron states at Ti sites. In fact, superpositions of partially occupied Ti t_{2g} orbitals producing their total charge equal to one, support the antiferromagnetic configurations.

One of the key factors which can intrinsically provide orbital disorder in $LaTiO_3$ is the spin-orbit coupling, not included in the basic nonrelativistic concept of altermagnetism. We note that this relativistic effect can induce spin-split bands due to noncollinear magnetism, as has recently been observed for a noncoplanar antiferromagnet $MnTe_2$ [27], making the studies of the relationship between altermagnetism and noncollinear magnetism and between altermagnetism and spin-orbit coupling very interesting [28].

The altermagnetic band structure of $LaTiO_3$ that we have calculated can shed light on various features of bulk $LaTiO_3$ and $LaTiO_3$-related heterostructures. First, its potentially anisotropic charge and spin transport properties can be modeled based on the calculated bandstructure. Second, the key element of the unit cell structure causing the Mott insulator behavior is the optimal tilting of the TiO_6 octahedra. This optimal structure realization is lifted at the $LaTiO_3/KTaO_3$ interfaces leading to the recently reported [26] emergence of interface symmetry-dependent two-dimensional conductivity and superconductivity. In this context, it would be worthwhile to investigate the role of altermagnetism in formation of the optimal tilting and, in turn, the interplay between the bulk altermagnetism and the formation of the interface-based electron states. An important finding is that small structural modifications of LTO can change the material from an altermagnet to a conventional magnetics allowing for the possibility of controllable switching of the spin-polarization of conduction electrons.

ACKNOWLEDGMENTS

The authors thank Igor Mazin for useful discussion. P.A.B. and A.E. acknowledge the funding by the Fonds zur Förderung der Wissenschaftlichen Forschung (FWF) under Grant No. I 5384. The work of E.S. is financially supported through the Grant No. PGC2018-101355-B-I00 funded by MCIN/AEI/10.13039/501100011033 and by ERDF "A way of making Europe," and by the Basque Government through Grant No. IT986-16.

[1] L. Šmejkal, J. Sinova, and T. Jungwirth, Phys. Rev. X **12**, 031042 (2022).
[2] I. Mazin, and The PRX Editors, Phys. Rev. X **12**, 040002 (2022).
[3] L.-D. Yuan and A. Zunger, Adv. Mater. **35**, 2211966 (2023).
[4] D. B. Litvin, Acta Cryst. A **33**, 279 (1977).
[5] L. Šmejkal, J. Sinova, and T. Jungwirth, Phys. Rev. X **12**, 040501 (2022).
[6] S. Bhowal and N. A. Spaldin, Phys. Rev. X **14**, 011019 (2024).
[7] L.-D. Yuan, Z. Wang, J.-W. Luo, and A. Zunger, Phys. Rev. Mater. **5**, 014409 (2021).
[8] M. Naka, Y. Motome, and H. Seo, Phys. Rev. B **103**, 125114 (2021).
[9] Z. Feng, X. Zhou, L. Šmejkal, L. Wu, Z. Zhu, H. Guo, R. González-Hernández, X. Wang, H. Yan, P. Qin *et al.*, Nat. Electron. **5**, 735 (2022).
[10] A. Bose and D. C. Ralph, Nat. Electron. **5**, 263 (2022).
[11] H. Bai, L. Han, X. Y. Feng, Y. J. Zhou, R. X. Su, Q. Wang, L. Y. Liao, W. X. Zhu, X. Z. Chen, F. Pan, X. L. Fan, and C. Song, Phys. Rev. Lett. **128**, 197202 (2022).
[12] S. Karube, T. Tanaka, D. Sugawara, N. Kadoguchi, M. Kohda, and J. Nitta, Phys. Rev. Lett. **129**, 137201 (2022).
[13] O. Fedchenko, J. Minár, A. Akashdeep, S. W. D'Souza, D. Vasilyev, O. Tkach, L. Odenbreit, Q. Nguyen, D. Kutnyakhov, N. Wind *et al.*, Sci. Adv. **10**, eadj4883 (2024).
[14] S. Lee, S. Lee, S. Jung, J. Jung, D. Kim, Y. Lee, B. Seok, J. Kim, B. G. Park, L. Šmejkal, C.-J. Kang, and C. Kim, Phys. Rev. Lett. **132**, 036702 (2024).
[15] J. Krempaský, L. Šmejkal, S. D'Souza, M. Hajlaoui, G. Springholz, K. Uhlířová, F. Alarab, P. Constantinou, V. Strocov, D. Usanov *et al.*, Nature (London) **626**, 517 (2024).
[16] I. V. Maznichenko, S. Ostanin, D. Maryenko, V. K. Dugaev, E. Y. Sherman, P. Buczek, I. Mertig, M. Kawasaki, and A. Ernst, Phys. Rev. Lett. **132**, 216201 (2024).
[17] B. Keimer, D. Casa, A. Ivanov, J. W. Lynn, M. v. Zimmermann, J. P. Hill, D. Gibbs, Y. Taguchi, and Y. Tokura, Phys. Rev. Lett. **85**, 3946 (2000).
[18] G. Khaliullin and S. Maekawa, Phys. Rev. Lett. **85**, 3950 (2000).
[19] M. Lüders, A. Ernst, M. Däne, Z. Szotek, A. Svane, D. Ködderitzsch, W. Hergert, B. L. Györffy, and W. M. Temmerman, Phys. Rev. B **71**, 205109 (2005).
[20] M. Geilhufe, S. Achilles, M. A. Köbis, M. Arnold, I. Mertig, W. Hergert, and A. Ernst, J. Phys.: Condens. Matter **27**, 435202 (2015).
[21] J. P. Perdew, K. Burke, and M. Ernzerhof, Phys. Rev. Lett. **77**, 3865 (1996).
[22] B. L. Gyorffy, Phys. Rev. B **5**, 2382 (1972).
[23] T. Oguchi, K. Terakura, and N. Hamada, J. Phys. F **13**, 145 (1983).

[24] B. Gyorffy, A. Pindor, J. Staunton, G. Stocks, and H. Winter, J. Phys. F **15**, 1337 (1985).

[25] V. I. Anisimov, J. Zaanen, and O. K. Andersen, Phys. Rev. B **44**, 943 (1991).

[26] D. Maryenko, I. Maznichenko, S. Ostanin, M. Kawamura, K. Takahashi, M. Nakamura, V. Dugaev, E. Y. Sherman, A. Ernst, and M. Kawasaki, APL Mater. **11**, 061102 (2023).

[27] Y.-P. Zhu, X. Chen, X.-R. Liu, Y. Liu, P. Liu, H. Zha, G. Qu, C. Hong, J. Li, Z. Jiang *et al.*, Nature (London) **626**, 523 (2024).

[28] M. Hajlaoui, S. W. D'Souza, L. Šmejkal, D. Kriegner, G. Krizman, T. Zakusylo, N. Olszowska, O. Caha, J. Michalička, A. Marmodoro, K. Výborný, A. Ernst, M. Cinchetti, J. Minar, T. Jungwirth, and G. Springholz, arXiv:2401.09187 [cond-mat.mtrl-sci].